Alkali activated materials based on glass waste and slag for thermal and acoustic insulation

S. Stoleriu, I. N. Vlasceanu, C. Dima, A. I. Badanoiu ✉, G. Voicu

Department of Science and Engineering of Oxide Materials and Nanomaterials, Faculty of Applied Chemistry and Materials Science, University Politechnica of Bucharest (Bucharest, Romania)
✉ alina.badanoiu@upb.ro

ABSTRACT: Porous alkali activated materials (AAM), can be obtained from waste glass powder and slag mixtures by alkali activation with NaOH solution. To obtain an adequate porous microstructure, the hardened AAM pastes were thermally treated at temperatures ranging between 900°C and 1000°C, for 60 or 30 minutes. Due to the intumescent behaviour specific for this type of materials, an important increase of the volume and porosity occurs during the thermal treatment.

The partial substitution of waste glass powder with slag, determines the increase of compressive strength assessed before (up to 37 MPa) and after (around 10 MPa) thermal treatment; the increase of slag dosage also determines the increase of the activation temperature of the intumescent process (above 950°C).

The high porosity and the specific microstructure (closed pores with various shapes and sizes) of these materials recommend them to be utilised as thermal and acoustical insulation materials.

KEYWORDS: Alkali activated materials; Foam; Glass-waste; Thermal and acoustical insulation.

RESUMEN: *Materiales activados alcalinamente a base de residuos de vidrio y escoria para aislamiento térmico y acústico*. Los materiales activados alcalinamente porosos (AAM) se pueden obtener a base de polvo de residuos de vidrio y mezclas de escoria mediante activación alcalina con una solución de hidróxido de sodio (NaOH). Para obtener una microestructura porosa adecuada, las pastas de AAM endurecidas se trataron térmicamente a temperaturas que oscilan entre 900°C y 1000°C durante 60 o 30 minutos. Debido al comportamiento intumescente específico de este tipo de material, se produce un aumento significativo en el volumen y la porosidad durante el tratamiento térmico. La sustitución parcial del polvo de residuos de vidrio por escoria conlleva un aumento en las resistencias a compresión previamente evaluadas (hasta 37 MPa) y después (aproximadamente 10 MPa) del tratamiento térmico; el aumento de la dosis de escoria también determina el aumento de la temperatura de activación del proceso intumescente (por encima de 950°C). La alta porosidad y la microestructura específica de estos materiales recomiendan que se utilicen como materiales de aislamiento térmico y acústico.

PALABRAS CLAVE: Materiales activados alcalinamente; Espuma; Residuos de vidrio; Aislamientos térmicos y acústicos.

ORCID ID: S. Stoleriu (https://orcid.org/0000-0003-3553-2034); I. N. Vlasceanu (https://orcid.org/0000-0001-8611-2027); C. Dima (https://orcid.org/0000-0003-1295-5034); A. I. Badanoiu (https://orcid.org/0000-0002-9091-3692); G. Voicu (https://orcid.org/0000-0001-7155-7138)

1. INTRODUCTION

Alkali activated materials, also known as geopolymers or inorganic-polymers, are products of the reaction between a solid component (powder) and an alkaline solution (1–3). According to Davidovits (1), these materials have a three-dimensional aluminate-silicate network, in which the tetrahedrons of $[SiO_4]^{4-}$ and $[AlO_4]^{5-}$ are connected and the electrical charge is balanced by the alkali cations.

The most common precursors used in the synthesis of alkali activated materials (AAM) are metakaolinite, slag and fly ash, but other waste such as ceramic tiles, red mud, rice husk ash, glass cullet and cathode ray tube glass can also be used as solid components (1–9).

AAM/geopolymer foams represent a new domain in research with high potential in producing thermal insulations (2, 10–15). The cellular structure specific for these materials can be achieved using foaming agents such as: hydrogen peroxide, sodium borates, metallic powders (Zn or Al), surfactants, carbonates or sodium silicate (10–16).

Our previous research focused on the synthesis of geopolymer foams based on waste glass (culet) with red mud slurry (waste resulted in bauxite processing industry) or fly ash (waste resulted in electrical power plants) additions (14). The results we obtained underlined the possibility of producing AAM /geopolymers by alkaline activation of silica-soda-lime waste glass (alone or with the above mentioned additions) with NaOH solution and thermal treatment at 60°C. The main compounds formed by the alkaline activation of these solid precursors are sodium silicate (aluminate) hydrates (7,14); these compounds, generated *in situ*, act as foaming agents during thermal treatment at temperatures ranging between 600–900°C (14). An important increase of the specimen's volume (and porosity) was achieved during the thermal treatment proving that these materials have an intumescent behaviour. The specific microstructure of thermally treated AAMs, based on waste glass powder with red mud or fly ash additions, i.e. closed pores with sizes ranging between 1–100 μm recommend them for the manufacturing of inorganic insulation materials.

It is well established that porous materials are good thermal and acoustical insulators. The thermal conductivity of porous geopolymers prepared by various processing methods (direct foaming, additive manufacturing or sacrificial filler method) is strongly influenced by the amount of open and closed pores, and can vary from 0.03 up to 0.88 W/m.K (17).

Whilst thermal properties have been widely studied, hardly any papers assess the sound absorption of geopolymer foams. The sound absorption coefficient of geopolymer foams based on fly ash and slag (18) or fly ash-geopolymeric concrete with construction and demolition waste as aggregate (19) can reach values raging between 0.6 and 1 in low frequency region (40–1000Hz); the sound absorption coefficient for these materials depends on several factors such as precursors nature, pore structure (open-closed) and distribution (17,18) and thickness of the specimen tested (17–19).

Research aiming to highlight waste glass as an alternative source for the traditional alkali activators based on alkali silicates was also carried out (20, 21); small amounts of waste glass powder were dissolved in $NaOH/Na_2CO_3$ solutions and used to prepared alkali activated materials based on slag (AAS) (20). The pastes mentioned above have a similar microstructure and strength as the alkali activated slag prepared with conventional sodium silicates solutions.

In this context, our study focuses on a different property of AAM based on waste glass powder with/without slag addition i.e. its ability to generate foams during thermal treatment; the main objective was to obtain thermal and acoustic insulation materials based on this type of AAM i.e. to establish the AAM compositions which subjected to thermal treatment (various temperatures and plateaus) can develop an adequate microstructure specific for a good thermal/acoustical insulation material. Beside the eco-friendly feature (waste recycling) a further important feature of these materials is their resistance to fire (non-combustible) due to the complete absence of organic components in their formula.

2. MATERIALS AND METHODS

The materials used for the synthesis of the alkali activated materials were:

- waste soda-lime-silica glass from a recycling facility; the waste glass (cullet) was grinded in a ball mill up to a fineness corresponding to a Blaine specific area of 2805 cm^2/g; the median diameter (D50) assessed by laser granulometry is 8.6 microns; the oxide composition of waste glass powder, assessed according to Romanian norms 5771-1-11-89 is: SiO_2 (68.5%), CaO (10.3%), Al_2O_3 (2.7%), Fe_2O_3 (2.5%), MgO (2.03%) and alkalis - Na_2O = 12.9% and K_2O=0.78 %. The density assessed with helium pycnometer is 2.5 g/cm^3.
- slag from a metallurgical plant; this industrial waste was also ground up to a fineness corresponding to a Blaine specific area of 3300 cm^2/g; the median diameter (D50) is 16.1 microns; the mineralogical components of slag, assessed by X ray diffraction (XRD), are: quartz - SiO_2, gehlenite - $Ca_2Al(AlSiO_7)$ and calcium silicate - Ca_2SiO_4. The density of slag is 2.83 g/cm^3.
- the alkaline activator was sodium hydroxide (chemical reagent).

The compositions of the alkali activated materials studied, are presented in Table 1. Slag substitutes various amounts of waste glass powder i.e. 5% wt., 10% wt. and 20% wt.

In order to increase the workability of fresh paste, for the compositions G_3 and G_3Z_{20}, the water amount was supplemented up to a water to solid ratio of 0.35.

NaOH pellets were dissolved in water and the solution was mixed with the solid component i.e. waste glass powder with/without slag addition. The resulting pastes were cast in rectangular moulds (15×15×60 mm) and cured at 60°C for 24h. The specimens were demoulded and cured in air at ambient temperature (20±2°C) for 7 days. The compressive strengths were assessed on paste specimens, using a Tonitech machine and the final value is calculated as the average of at least four strength values assessed on specimens cured in the same conditions.

The hardened specimens were thermally treated at temperatures ranging between 900°C and 1000°C, for 60 or 30 minutes; the heating rate (up to the maximum temperature of 900°C, 950°C and 1000°C) was 10°C/minute. For G_3 and G_3Z_{20} the thermal treatment temperatures and plateau were selected based on the results obtained for the G_2 series.

SEM and EDX analyses were performed on paste specimens (fracture surfaces) coated with Ag, using a HITACHI S 2600 N microscope.

The XRD analysis of slag was performed on a Shimadzu XRD 6000 diffractometer. The XRD patterns were obtained using a monochromatic CuKα radiation (λ = 1.5406 Å), range 2θ from 5 to 50 degrees.

The apparent density (ρ_a) and open porosity (P_o) were assessed on the thermally treated specimens employing the immersion method, using as liquid medium xylene (ρ_{xylene} = 0.86 g/cm^3) (22). The density (ρ) was assessed with a helium pycnometer. Total porosity (P_t) was calculated with the following formula [1] (23):

$$P_t = (1 - \rho_a/\rho) \cdot 100 \ (\%) \qquad [1]$$

The mass change of specimens after the thermal treatment was calculated with the following formula [2]:

$$\Delta m = [(m_a - m_b)/m_b] \cdot 100 \ (\%) \qquad [2]$$

where: m_b = mass before thermal treatment; m_a = mass after thermal treatment.

Short term water absorption by partial immersion of specimen, was determined on selected compositions i.e. G_3 and G_3Z_{20}; the test specimens i.e. cuboids (50 × 50 × 30 mm) were kept before testing for at least 6 hours at 23±5°C.

Short term water absorption by partial immersion, (W_p) was calculated according to EN 1609 (24) with the following formula [3]:

$$W_p = (m_{24} - m_0) / A_p \ (kg/m^2) \qquad [3]$$

where: m_0 = initial mass of the test specimen (kg); m_{24} = mass of the test specimen after partial immersion in water for 24 hours (kg); A_p = bottom surface area of the test specimen (m^2).

The coefficient of thermal expansion was assessed with a dilatometer DIL 402 Netzch. The analysis was performed on specimens with 15.6±0.3 mm lengths, in the temperature range 20–600°C with a heating rate of 3K/min.

Thermal conductivity was assessed using a thermal conductivity analyzer, HESTO - Lambda-CONTOL A90, in accordance with EN 12667 (25). The test specimens were boards (300×300×30 mm); the specimens were kept before the test for at least 6 hours at 23 ± 5°C.

The compressive strength at 10% deformation was assessed on a testing machine (Tinius Olsen); test specimens – boards (100×100×30 mm), were kept before the test for at least 6 hours at 23 ± 5°C, in accordance with EN 826 (26).

The determination of the acoustic absorption coefficient (α) was achieved by the Kundt tube method according to EN ISO 10534-1: 2002 (27) and EN ISO 10534-2: 2005 (28) on discs with a nominal diameter of 63.5 mm and a thickness of 15 mm at a temperature of 26°C and a relative humidity of 58%.

The test specimens used for the assessment of short term water absorption by partial immersion, thermal conductivity, compressive strength at 10% deformation and acoustic absorption coefficient were cut from the thermally treated specimens.

3. RESULTS AND DISCUSSIONS

The influence of the water to solid ratio and slag dosage on the compressive strengths values is presented in Figure 1. For all the compositions studied,

TABLE 1. Compositions (%wt) of studied alkali activated materials

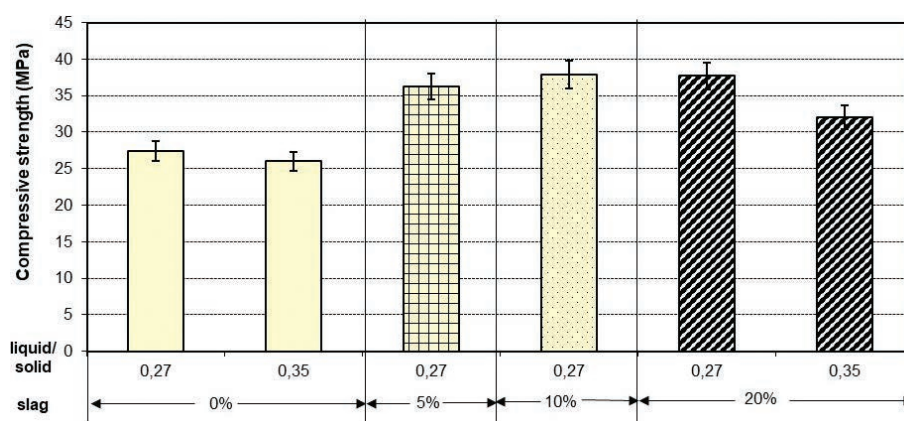| Specimen	Waste glass	Slag	NaOH	Water/solid Ratio
G_2	93.3	-	6.7	0.27
G_2Z_5	88.8	4.5	6.7	0.27
G_2Z_{10}	84.3	9	6.7	0.27
G_2Z_{20}	75.3	18	6.7	0.27
G_3	93.3	-	6.7	0.35
G_3Z_{20}	75.3	9	6.7	0.35

Figure 1.   Influence of slag amount and water to solid ratio on the compressive strength.

the values of compressive strengths (before thermal treatment) are high (over 25 MPa); the increase of slag amount determines the increase of compressive strength for the specimens prepared with a lower amount of water (water to solid ratio = 0.27). This can be explained by the formation of calcium aluminate silicate hydrates (C-A-S-H) resulted in the activation of slag hydration process in alkaline solution (29).

The thermal treatment of these specimens determines important volume and porosity value increases (intumescent behaviour). As it can be seen from Table 2, a higher volume increase is recorded for the alkali activated materials without slag (G_2 and G_3) when the thermal treatment is performed at 900°C for 60 minutes. The increase of water to solid ratio from 0.27 (G_2) to 0.35 (G_3) determines the apparition of deep cracks in the specimen, most probably caused by the moisture loss during the rapid heating of the specimens in the oven.

The increase of slag dosage determines the increase of the activation temperature for the intumescent effect i.e. the highest volume increase was recorded at 950°C for the AAMs with 5%wt. and 10%wt. slag and at 1000°C for those with 20%wt. slag (G_2Z_{20}). This can be due to the presence in the slag of crystalline compounds, such as quartz and gehlenite, with high melting points (above 1590°C) (30).

The influence of thermal treatment on the compressive strengths of alkali activated materials is presented in Figure 2. As expected, the increase of specimens' volume and porosity (see Tables 2 and 3) determines the decrease of the compressive strength. However, it is interesting to note the high values achieved for G_2 and G_2Z_{10} compositions (around 10 MPa) after the thermal treatment at 900°C/60 minutes.

The influence of thermal treatment on the mass changes, apparent density, open and total porosities porosity of the alkali activated materials is presented in Table 3. One can notice an important decrease of the apparent density after the thermal treatment, due to an important increase of the volume in conjunction with mass loss (Δm) – 16–18%. The mass loss (table 3) and volume increase (Table 2) explain the important decrease of apparent density of thermally treated specimens from 2.03–2.20 g/cm^3 (before thermal treatment) to values around 1 g/cm^3 and even smaller (below 0.86 g/cm^3 for the specimen G_3 thermally treated at 900°C for 60 minutes – Table 3).

The thermal treatment also determines an increase of open and total porosity of these materials; the important gap between the open and total porosity values it is due to the specific microstructure of this type of materials i.e. closed pores with various sizes and shapes (see Figs. 3 and 4); additionally, the thermal treatment determines a "self-glazing effect", further reducing the open pores (see also Table 2).
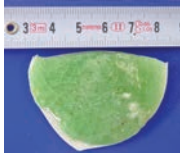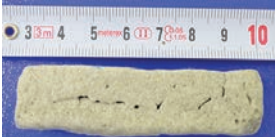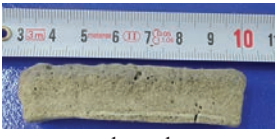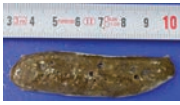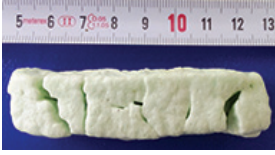
The microstructure of G_3 specimen, before and after thermal treatment at 900°C, for 60 minutes is presented in Figure 3.

In the SEM micrograph of G_3 specimen, before thermal treatment (Figure 3a,c), the binding matrix resulted in the reaction of NaOH solution with waste glass powder, can be assessed (7). One can notice the presence of round closed pores (Figure 3a). These pores are most probably determined by the air entrapped during the mixing of the solid component (powder glass) with NaOH solution.

On the SEM micrograph of G_3, after the thermal treatment, a large number of pores with various forms and sizes are present; these pores are formed during the water loss and transformation of sodium silicate (aluminate) hydrates resulting from the reaction of waste glass powder and NaOH solution (7, 14).

On the SEM micrographs of the specimen with 20% slag (G_3Z_{20}), before thermal treatment (Figure 4a), one can also assess the round pores formed by

TABLE 2.   Visual aspect of alkali activated materials before/after thermal treatment at temperatures ranging between 900° and 1000°C

Sample code	Water to solid ratio	Before thermal treatment	900°C/60 min	950°C/30 min	1000°C/60 min
G_2	0.27				
G_2Z_5	0.27				
G_2Z_{10}	0.27		lateral		
G_2Z_{20}	0.27				
G_3	0.35				
G_3Z_{20}	0.35				

entrapped air during mixing of the solid component with the sodium solution. After the thermal treatment, on the micrograph presented in Figure 4b, the presence of large pores and small round pores can be noticed (see arrows) in the walls of these large pores.

The high porosity and the specific microstructure (closed pores with various shapes and sizes) of these AAMs recommend them to be utilized as insulation materials.

In Table 4 we present the values of some of the properties specific for insulating materials assessed in accordance with European norms (EN) for the composition G_3 and G_3Z_{20} thermally treated at 900°C for 60 minutes.

The thermal conductivity assessed for these AAMs are comparable with the values assessed on thermal insulation based on cellular glass i.e. 0.05 – 0.08 (W/m·K).

The values of compressive strengths at 10% deformation of alkali activated materials (G_3 and G_3Z_{20}) are smaller compared with those specific for other types of commercial insulating materials such as extruded (150–700 kPa) and expanded polystyrene (70–260 kPa) (31) or mineral wool (2.4–104 kPa) (32, 33), because AAMs are brittle materials. Nevertheless, these values are higher in comparison with those assessed for glass wool (0.21–16.6 kPa) (32, 33).
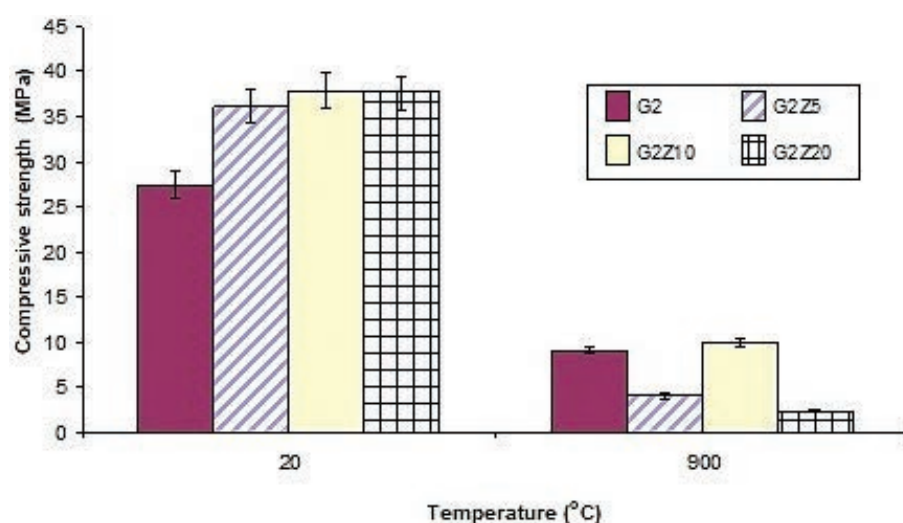
FIGURE 2. Influence of thermal treatment at 900°C/1 h on the compressive strength of AAMs.

TABLE 3. Apparent density, open and total porosities and mass loss of studied alkali activated materials

Comp.	Temperature (°C)	Time (min)	Mass loss (Δm) (%)	Apparent density (ρ_a) (g/cm^3)	Open porosity (P_o) (%)	Total porosity (Pt) (%)
G_2	Initial		-	2.2	7.13	-
	900	60	-18.08	-	15.17	68.12
G_2Z_5	Initial		-	2.09	1.25	4.70
	900	60	-18.01	1.07	11.3	55.83
	950	30	-16.82	0.97	10.44	58.61
G_2Z_{10}	Initial		-	2.08	2.34	5.89
	900	60	-18.07	1.25	12.72	55.83
	950	30	-17.10	1.03	9.45	58.87
G_2Z_{20}	Initial		-	2.03	3.44	9.86
	950	30	-16.32	0.99	14.73	59.96
	1000	60	-16.95	1.02	13.59	58.92
G_3	Initial		-	2.12	1.82	3.07
	900	60	-16.77	<0.86*	-	-
G_3Z_{20}	Initial		-	2.05	3.24	7.61
	900	60	-17.46	1.17	16.55	51.65
	950	30	-16.60	1.01	16.89	58.37

* specimen floats on xylene

The water absorption by partial immersion after a short time for G_3 slightly exceeds the limit value of 1 kg/m^2. The higher value assessed on G_3Z_{20} specimen can be due to the presence of bigger pores/cracks (see also Table 2) which appeared during the thermal treatment.

The values of thermal expansion coefficients for G_3 and G_3Z_{20} are similar to values specific for cellular glass ($8 \div 10 \times 10^{-6}$ K^{-1}(34)). This demonstrates a good thermal stability of these compositions and

recommends them (along with the thermal conductivity values) to be used as thermal insulating materials. Furthermore, because these AAMs do not contain organic phases, they can be classified as fire resistant materials - Euroclass A1 (34).

The sound absorption coefficient (α) defined as the ratio of the sound intensity absorbed by the material and the intensity of incident sound, should have high values for efficient sound absorbing materials. The behaviour of sound absorption coefficient vs.
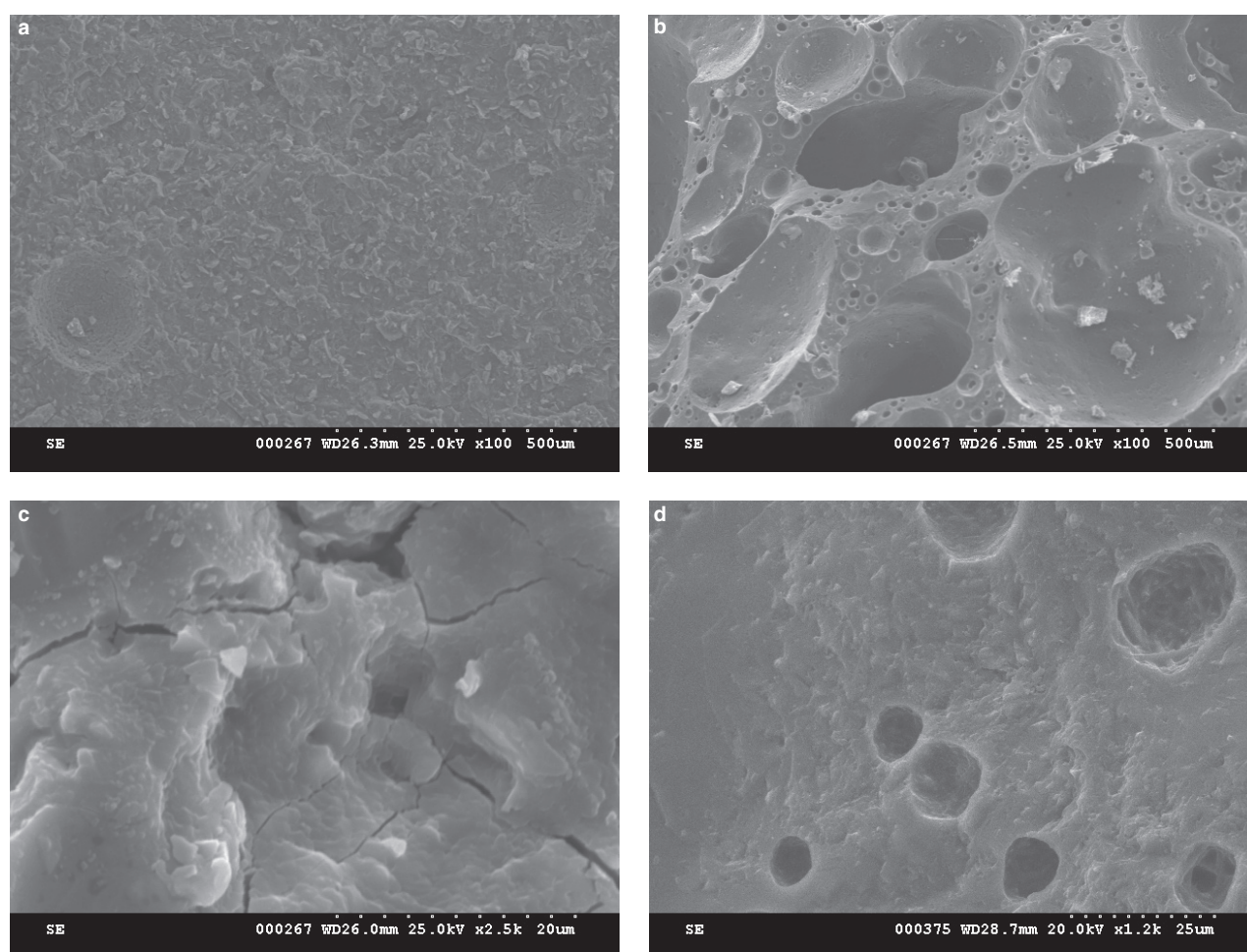
FIGURE 3.   SEM micrographs of G_3 specimen before (a, c) and after thermal treatment (900°C/60 min.) (b, d).

TABLE 4.   Properties of alkali activated materials after thermal treatment at 900°C for 60 minutes

Property (U.M)	EN norm	G_3	G_3Z_{20}
Thermal conductivity (W/m·K)	EN 12667	0.0748	0.0788
Compressive strength at 10% deformation (kPa)	EN 826	32.94	59.85
Short term water absorption by partial immersion (kg/m^2)	EN 1609	1.53	3.25
Coefficient of thermal expansion 20–300°C (10^{-6}.K^{-1})	-	11.04	9.77

the frequency of incident sound for these materials is presented in Figure 5. As it can be observed, the best acoustic performance of these materials is achieved at frequencies ranging between 1200–1600Hz; the maximum absorption coefficient recorded for G_3 is 0.98 and for G_3Z_{20} is 1 (Figure 5).

The good acoustic properties of these materials (in the frequencies range 1200–1600Hz) are explained by their high porosity (see table 3). It should also be noticed that specimens used for this analysis were obtained by cutting from the thermally treated specimens, i.e. removing the superficial vitreous layer (resulted due to "self glazing effect"); this processing increases the surface of specimens in contact with the sound wave (due to the high number of pores exposed at the surface) which is an important factor in the sound mitigation (35, 36).

4. CONCLUSIONS

Alkali activated materials (AAM) with intumescent properties were obtained using waste glass powder and NaOH solution. In some compositions slag
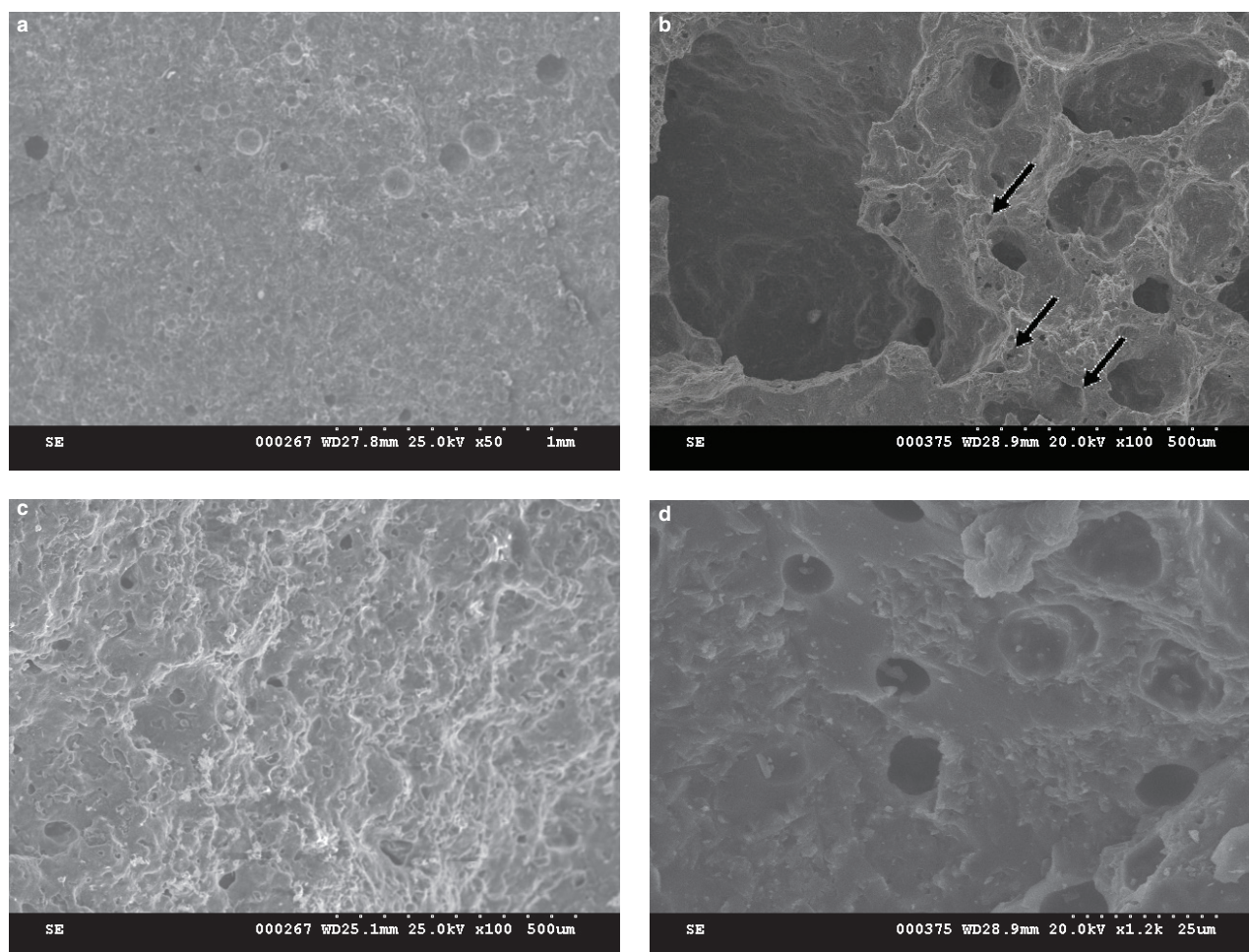
FIGURE 4.   SEM micrographs of G_3Z_{20} specimen before (a, c) and after thermal treatment (900°C/60 min.) (b, d).

FIGURE 5.   Sound absorption coefficient vs. sound frequency: a) G_3 and b) G_3Z_{20}.

was added in various amounts (5%wt. up to 20%wt. as glass powder substitute).

The values of compressive strengths, prior to thermal treatment, are over 25 MPa for all the AAMs studied. The increase in slag amount determines the increase in compressive strength for the specimens prepared with a lower amount of water (w/s=0.27).

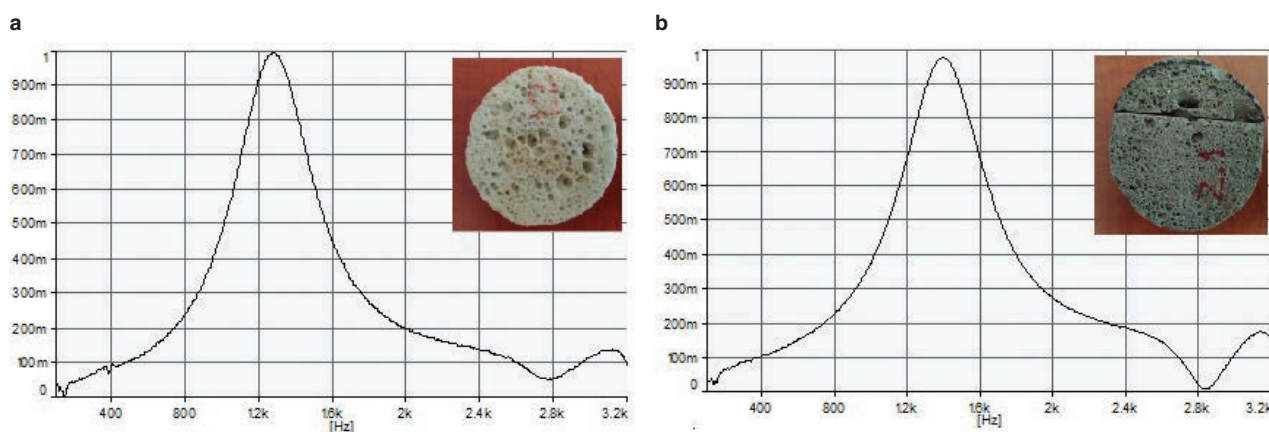The thermal treatment determines an important swelling of specimens (intumescent behaviour). As expected, due to the important increase in the porosity, the compressive strength decreases; however, for some compositions (G_2 and G_2Z_{10}), the values of compressive strengths remain quite high (around 10 MPa).

The thermally treated specimens have a self-glazing effect (thus a low open porosity) and their microstructure consist in closed pores with various sizes and shapes. These pores are the result of water loss and transformation of sodium/calcium silicate (aluminate) hydrates derived from the reaction of glass powder/slag with NaOH solution.

The values of thermal conductivity of AAMs (G_3 and G_3Z_{20}), thermally treated at 900°C with a 60 minutes plateau, are comparable with the values assessed on thermal insulation based on cellular glass. The AAMs studied also have thermal expansion coefficients comparable with those specific for cellular glass, demonstrating a good thermal stability, an important feature (along with thermal conductivity) if these materials are used for the purpose of thermal insulation.

The best acoustic performances of such materials are achieved at frequencies ranging between 1200–1500Hz; the maximum absorption coefficient recorded for G_3 is 0.98 and for G_3Z_{20} is 1.

Additionally, due to the fact the AAMs studied do not contain organic phases, these materials can be classified as fire resistant - Euroclass A1.

ACKNOWLEDGEMENTS

REFERENCES

1. Davidovits, J. (2008) Geopolymer Chemistry and Applications, Saint-Quentin: Institute Géopolymère, (2008)
2. Pacheco-Torgal, F.; Labrincha, J.; Leonelli, C.; Palomo, A.; Chindaprasit, P. (2015) Handbook of Alkali-Activated Cements, Mortars and Concretes, Elsevier.
3. Torres-Carrasco, M.; Puertas, F. (2017) Alkaline activation of aluminosilicates as an alternative to portland cement: a review, *Rom. J. Mater.* 47 (1), 3–15.
4. Cyr, M.; Idir, R.; Poinot, T. (2012) Properties of inorganic polymer (geopolymer) mortars made of glass cullet, *J. Mater. Sci.* 47, 2782–2797. https://doi.org/10.1007/s10853-011-6107-2
5. Sun, Z.; Cui, H.; An, H.; Tao, D.; Xu, Y.; Zhai, J.; Li, Q. (2013) Synthesis and thermal behavior of geopolymer-type material from waste ceramic, *Constr. Build. Mater.* 49, 281–287. https://doi.org/10.1016/j.conbuildmat.2013.08.063
6. Rashidian-Dezfouli, H.; Rangaraju, P. R. (2017) Comparison of strength and durability characteristics of a geopolymer produced from fly ash, ground glass fiber and glass powder, *Mater. Construcc.* 67 [328], e136. https://doi.org/10.3989/mc.2017.05416
7. Badanoiu, A.; Al Saadi, T.; Voicu, G. (2015) Synthesis and properties of new materials produced by alkaline activation of glass cullet and red mud, *Int. J. Miner. Process.* 135, 1–10. https://doi.org/10.1016/j.minpro.2014.12.002
8. Al Saadi, T.; Badanoiu, A.; Voicu, G.; Stoleriu, S. (2015) Effect of alkaline activator on the main properties of geopolymers based on cullet glass and red mud, *Rom. J. Mater.* 45, 138–146.
9. Villaquirán-Caicedo, M.A.; Mejía de Gutiérrez, R.; Gallego, N.C. (2017) A Novel MK-based Geopolymer Composite Activated with Rice Husk Ash and KOH: Performance at High Temperature, *Mater. Construcc.* 67 [326], e117. https://doi.org/10.3989/mc.2017.02316
10. Abdollahnejad, Z.; Pacheco-Torgal, F.; Félix, T.; Tahri, W.; Barroso Aguiar, J. (2015) Mix design, properties and cost analysis of fly ash-based geopolymer foam, *Constr. Build. Mater.* 80, 18–30. https://doi.org/10.1016/j.conbuildmat.2015.01.063
11. Masi, G.; Rickard, W.D.A.; Vickers, L.; Bignozzi, M.C.; van Riessen, A. (2014) A comparison between different foaming methods for the synthesis of light weight geopolymers, *Ceram. Int.* 40, 13891–13902. https://doi.org/10.1016/j.ceramint.2014.05.108
12. Guo, Y.; Zhang, Y.; Huang, H.; Meng, K.; Hu, K.; Hu, P.; Wang, X.; Zhang, Z.; Meng, X. (2014) Novel glass ceramic foams, materials based on red mud, *Ceram. Int.* 40, 6677–6683. https://doi.org/10.1016/j.ceramint.2013.11.128
13. Chen, X.; Lu, A.; Qu, G. (2013) Preparation and characterization of foam ceramics from red mud and fly ash using sodium silicate as foaming agent, Ceram. Int., 39, 1923–1929, https://doi.org/10.1016/j.ceramint.2012.08.042
14. Badanoiu, A.; Al Saadi, T.; Stoleriu, S.; Voicu, G. (2015) Preparation and characterization of foamed geopolymers from waste glass and red mud, *Constr. Build. Mater.* 84, 284–293. https://doi.org/10.1016/j.conbuildmat.2015.03.004
15. Bai, C.; Ni, T.; Wang Q.; Li, H; Colombo, P. (2018) Porosity, mechanical and insulating properties of geopolymer foams using vegetable oil as the stabilizing agent, *J. Eur. Ceram. Soc.* 38 [2], 799–805. https://doi.org/10.1016/j.jeurceramsoc.2017.09.021
16. Al Saadi, T.; Badanoiu, A.I.; Nicoara, A.I.; Stoleriu, S.; Voicu, G. (2017) Synthesis and properties of alkali activated borosilicate inorganic polymers based on waste glass, *Constr. Build. Mater.* 136, 298–306, https://doi.org/10.1016/j.conbuildmat.2017.01.026
17. Bai, C.; Colombo, P. (2018) Processing, properties and applications of highly porous geopolymers: A review, *Ceram. Int.* 44, 16103–16118, https://doi.org/10.1016/j.ceramint.2018.05.219
18. Zhang, Z.; Provis, J.L.; Reid, A.; Wang, H. (2015) Mechanical, thermal insulation, thermal resistance and acoustic absorption properties of geopolymer foam concrete, *Cem. Concr. Compos.* 62, 97–105, https://doi.org/10.1016/j.cemconcomp.2015.03.013
19. Arenas, C.; Luna-Galiano, Y.; Leiva, C.; Vilches, L.F.; Arroyo, F.; Villegas, R.; Fernández-Pereira, C. (2017) Development of a fly ash-based geopolymeric concrete with construction and demolition wastes as aggregates in acoustic barriers, *Constr. Build. Mater.* 134, 33–442. https://doi.org/10.1016/j.conbuildmat.2016.12.119
20. Torres-Carrasco, M.; Palomo, J. G.; Puertas, F. (2014) Sodium silicate solutions from dissolution of glass wastes. Statistical analysis, *Mater. Construcc.* 64 [314], e014. https://doi.org/10.3989/mc.2014.05213
21. Puertas, F.; Torres-Carrasco, M. (2014) Use of glass waste as an activator in the preparation of alkali-activated slag. Mechanical strength and paste characterization, *Cem. Concr. Res.* 57, 95–104. https://doi.org/10.1016/j.cemconres.2013.12.005
22. ISO 10545-3:1995, Ceramic tiles - Part 3: Determination of water absorption, apparent porosity, apparent relative density and bulk density.
23. Barbosa, A. R. J.; Lopes, A. A. S.; Sequeira, S. I. H; Oliveira, J. P.; Davarpanah, A.; Mohseni, F.; Amaral, V. S.; Monteiro, R. C (2016) Effect of processing conditions on the properties of recycled cathode ray tube glass foams, *J. Porous Mater.* 23, 1663–1669. https://doi.org/10.1007/s10934-016-0227-7

24. EN 1609 – Thermal insulating products for building applications – Determination of short term water absorption by partial immersion

25. EN 12667 - Thermal performance of building materials and products – Determination of thermal resistance by means of guarded hot plate and heat flow meter methods - Products of high and medium thermal resistance

26. EN 826 - Thermal insulating products for building applications – Determination of compression behavior

27. EN ISO 10534-1:2002 Acoustics - Determination of sound absorption coefficient and impedance in impedance tubes -- Part 1: Method using standing wave ratio

28. EN ISO 10534-2:2005 - Acoustics - Determination of sound absorption coefficient and impedance in impedance tubes -Part 2: Transfer-function method

29. Duxson, P.; Fernández-Jiménez, A.; Provis, J.L.; Lukey, G.C.; Palomo, A.; van Deventer, J.S.J. (2007) Geopolymer technology: the current state of the art, *J. Mater. Sci.* 42, 2917–2933. https://doi.org/10.1007/s10853-006-0637-z

30. Osborn, E.F.; Muan, A. (1960) Revised and redrawn "Phase equilibrium diagrams of oxide systems", Plate 3 - System MgO-Al$_2$O$_3$-SiO$_2$, American Ceramic Society and the Edward Orton, Jr. Ceramic foundation, (1960)

31. Winterling H.; Sonntag N., (2011) Rigid Polystirene Foam (EPS, XPS), Kunststoffe International, 10, 18–21.

32. Strother, E.F. and Turner, W.C. (1990) Thermal Insulation Building Guide, Robert E. Krieger Publishing Company, ISBN-10: 088275985X (1990)

33. Veiseh S.; Mirmohamadi M.M.; Khodabandeh N.; Hakkaki-Farda A. (2007) Assessment of parameters affecting compressive behavior of mineral wool insulations, *Asian J. Civ. Eng.* 8[4], 359–373

34. EN 13167+A1:2015 - Thermal insulation products for buildings - Factory made cellular glass (CG) products – Specification

35. Elkhessaimi, Y.; Tessier-Doyen N.; Smith, A (2017) Effects of microstructure on acoustical insulation of gypsum boards, *J. Build. Eng.* 14, 24–31. https://doi.org/10.1016/j.jobe.2017.09.011

36. Ghizdaveț, Z.; Ștefan B.M.; Nastac, D.; Vasile,O.; Bratu, M. (2016) Sound absorbing materials made by embedding crumb rubber waste in a concrete matrix, Constr. Build. Mater., 124, 755–763. https://doi.org/10.1016/j.conbuildmat.2016.07.145